Elliptical Polarization Favors Long Quantum Orbits in High-Order Above-Threshold Ionization of Noble Gases

XuanYang Lai,[1] ChuanLiang Wang,[1,2] YongJu Chen,[1,2] ZiLong Hu,[1,2] Wei Quan,[1] and XiaoJun Liu[1,*]

[1]*State Key Laboratory of Magnetic Resonance and Atomic and Molecular Physics, Wuhan Institute of Physics and Mathematics, Chinese Academy of Sciences, Wuhan 430071, China*

[2]*Graduate School of Chinese Academy of Sciences, Beijing 100080, China*

Jing Chen[†]

HEDPS, Center for Applied Physics and Technology, Peking University, Beijing 100084, China and Institute of Applied Physics and computational Mathematics, P. O. Box 8009, Beijing 100088, China

Ya Cheng and ZhiZhan Xu

State Key Laboratory of High Field Laser Physics, Shanghai Institute of Optics and Fine Mechanics, Chinese Academy of Sciences, P. O. Box 800-211, Shanghai 201800, China

Wilhelm Becker

Max Born Institute for Nonlinear Optics and Short-Pulse Spectroscopy, Max-Born-Strasse 2a, 12489 Berlin, Germany

(Received 4 July 2012; published 23 January 2013)

We demonstrate the significant role of long quantum orbits in strong-field atomic processes by investigating experimentally and theoretically the above-threshold ionization spectra of noble gases in intense elliptically polarized laser pulses. With increasing laser ellipticity, the yields of different energy regions of the measured electron spectrum in high-order above-threshold ionization drop at different rates. The experimental features can be reproduced by a theoretical simulation based on quantum-orbit theory, revealing that increasing ellipticity favors the contributions of the long quantum orbits in the high-order above-threshold ionization process.

DOI: 10.1103/PhysRevLett.110.043002 PACS numbers: 32.80.Rm, 32.80.Wr, 42.50.Hz

When an intense laser field (with an intensity $I \gtrsim 10^{13}$ W/cm^2) interacts with an electron bound in an atom or molecule, the fundamental process to occur is ionization. Owing to its very highly nonlinear character, this has attracted the attention of experimentalists and theorists alike since the early work of Agostini [1]. If the electron, liberated and subsequently driven by the laser field, revisits its parent ion, this results in various additional highly nonlinear phenomena [2], such as high-order above-threshold ionization (HATI) [3], high-order harmonic generation (HHG) [4], nonsequential double ionization (NSDI) [5], and population of high-lying Rydberg states [6]. Once the electron is free, the competition between the forces exerted by the laser field and by the binding potential is decided in favor of the former. Then, except at the brief instances when the electron revisits its parent ion, the physics is largely classical, while the very first step, the process of ionization itself, is quantum mechanical.

A theoretical framework ideally suited to this situation is the formalism of quantum orbits, which results from a saddle-point evaluation of the ionization amplitude in the strong-field approximation (SFA) [7,8]. The real part of a quantum orbit is much like a classical trajectory in the presence of the laser field. There is an imaginary part, too, which is related to the origin of the quantum orbit through tunneling and to the tunneling rate. It is comparatively small except when a quantum orbit accesses territory that is classically inaccessible; in that case the real and imaginary parts become comparable. If more than one quantum orbit connects a given initial and final state, their contributions interfere, generating a pronounced beating pattern. Apart from a numerical solution of the time-dependent Schrödinger equation, which may be very time consuming and does not reveal much of the underlying physics, quantum orbits arguably provide the best combination of accuracy and physical insight.

Quantum orbits are best known from the theory of high-order harmonic generation, where the so-called "long orbit" and the "short orbit" contribute, in principle, to any given harmonic [9] although their relative importance for the collective response depends on the focusing conditions. However, there are additional orbits, called the "longer orbits." This refers to orbits that travel for a longer time between ionization and recombination than the former two. They are a straightforward consequence of the saddle-point evaluation and are responsible for the fine structure of, e.g., the harmonic plateau [10,11]. But in experiments so far unambiguous imprints of the longer orbits have been difficult to isolate; in fact, even the interference of the common short and long orbits has been observed only recently [12], and the interplay between macroscopic (e.g., phase matching) and microscopic effects

inherent in HHG still frustrates a clear separation of the various quantum orbits [13]. In contrast, HATI spectra, which exhibit the single-atom response to the intense laser pulse, are not subject to these complications and allow for a much more straightforward identification of the effects of the longer orbits. Indeed, they impressively exhibit the so-called intensity-dependent enhancements, which can be explained by constructive interference of many longer orbits on the single-atom level [14–16].

For elliptical polarization it is known from theory that with increasing ellipticity contributions of the longer orbits become more significant, giving the spectrum the appearance of a "staircase" for large ellipticity [17]. However, in experiments up to now it has not been possible unambiguously to attribute certain features of the spectrum to the dominance of the longer orbits. On the other hand, it is becoming increasingly important to understand the ellipticity aspects of strong-field atomic processes considering that elliptical polarization has great significance as a tool, for example, for attosecond temporal gating [18] and by providing the "minute hand" of the "attoclock" [19].

In this Letter, we present above-threshold ionization (ATI) spectra along the major polarization axis for the three rare gases Ar, Kr, and Xe up to ellipticities of $\xi = 0.36$, recorded with 25-fs pulses of 800 nm central wavelength and intensities in the upper 10^{13} W/cm^2. By comparing the relative ellipticity dependence of various energy regions of the HATI spectra, we are able to distinguish the contributions from different orbits and thus to provide clear evidence for the significance of quantum orbits beyond the well established "short" and "long" orbit.

In our experiments, the laser pulses are generated by a 5 kHz femtosecond Ti:sapphire laser system (Femtopower Compact Pro Amplifier, FEMTOLASERS Produktions GmbH). The laser-pulse energy can reach 0.8 mJ with a pulse duration of 25 fs and a central wavelength of 800 nm. The photoelectron energy spectra are detected by using a homemade field-free time-of-flight (TOF) spectrometer. The base pressure of the spectrometer is maintained below 2×10^{-9} mbar and the sample gases are fed into the interaction chamber through a leak valve. The sample gas pressure in the chamber varies from 10^{-6} to 10^{-8} mbar, depending on the gas species and laser ellipticity. Photoionized electrons are detected by microchannel plates with a collecting angle of 5° and are recorded by a multihit time-to-digital converter with an ultimate resolution of 25 ps (TDC8HP, Roentdek Handels GmbH). The ellipticity of the laser polarization is controlled by rotating a quarter wave plate right before the incident window, and the major axis of the laser field is kept along the direction of the photoelectron detector as the ellipticity changes while the intensity is constant. The high detection sensitivity together with the high laser repetition rate allow recording HATI spectra with high efficiency and covering the entire rescattering plateau up to and beyond its cutoff, even for high ellipticity.

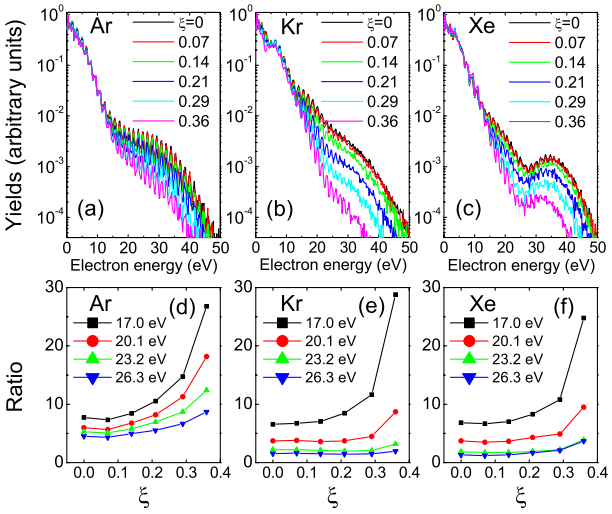

FIG. 1 (color online). Experimental [(a), (b), and (c)] photoelectron spectra of Ar, Kr, and Xe along the major polarization axis for elliptically polarized laser pulses with wavelength of 800 nm, intensity of 7.0×10^{13} W/cm^2, and ellipticities $\xi = 0$, 0.07, 0.14, 0.21, 0.29, and 0.36 from top to bottom. The spectra are normalized to unity at zero energy. (d), (e), (f) Ratios of the electron yields for various low-energy intervals over one high-energy interval as functions of the ellipticity. For details, see the text.

Figures 1(a)–1(c) exhibit the photoelectron spectra of Ar, Kr, and Xe along the major polarization axis for ellipticities between $\xi = 0$ and $\xi = 0.36$. All spectra have been normalized to unity at zero energy thus compensating the decrease of the yield of direct electrons for increasing ellipticity, which corresponds to the field amplitude dropping as $E_0/\sqrt{1 + \xi^2}$. As a result, the spectrum of the direct electrons (normalized as mentioned) is all but independent of the ellipticity. (Of course, this will change for ellipticities higher than we consider in this Letter, when for about $\xi > 0.5$ the transition to the typical spectrum of circular polarization will set in.)

We draw attention to several prominent features of these spectra. A very noticeable effect is the extremely well-defined departure from the afore-mentioned ellipticity-independent exponential dropoff of the direct-electron spectrum to a pronounced ellipticity dependence, which roughly happens at the energy where rescattering electrons start to dominate the direct ones. At this point, the spectra for the various ellipticities suddenly start to fan out. The transition energy is particularly well defined for argon at 12–13 eV corresponding to $3.0U_p$ for the estimated peak intensity of 7.0×10^{13} W/cm^2 ($U_p = 4.2$ eV; U_p denotes the ponderomotive energy of the laser field). This property may provide a tool to calibrate the peak intensities of different experiments. Above the transition point just discussed, the rescattering plateau sets in, which with increasing ellipticity more and more turns into an inclined plane. The ellipticity-dependent classical cutoff is located at

approximately $10.01U_p/(1+\xi^2)$ [20]. The plateaus of Figs. 1(a)–1(c) display a very pronounced species dependence in close agreement with the data of Ref. [21] for linear polarization.

Before we turn to a detailed theoretical analysis of the spectra and demonstrate the significant role of the long orbits in HATI, we will give a brief summary of the concept of quantum orbits [11,22]. To a remarkable extent, rescattering processes can be understood in terms of classical electron trajectories, which are driven only by the laser field. The trajectories start at certain times t at the "exit of the tunnel." At later times, the electron may revisit its parent ion, at which time it may scatter elastically. Only a single act of rescattering is taken into account, but this does not necessarily take place at the first revisit. Namely, the electron may also, at this time, ignore the ion and instead rescatter on the second revisit, or on the third, or at some later visit. For given final electron momentum $\mathbf{p}$, there is one pair of orbits that scatter on the first revisit, another one whose orbits scatter on the second revisit, and so on, for so long as the laser pulse lasts. The trajectories of the nth pair have a certain cutoff energy, that is, they can only reach a certain maximal energy $E_{c,n}$, so that $\mathbf{p}^2/2 < E_{c,n}$. For the first pair, this is the well-known energy of $10.01U_p$, for the second and the third pair, the cutoff energies are $7.1U_p$ and $8.75U_p$ [11]. At these cutoff energies, the two orbits of the respective pair merge.

Quantum mechanics adds essentially two features to this classical picture: the start times become complex in a fashion to be explained below, and the contributions of the various orbits, that is, their *amplitudes*, have to be added coherently. In consequence, the contributions of different orbits interfere.

For linear polarization, the first pair is dominant for electrons with very high kinetic energy, i.e., with energy close to the $10.01U_p$ HATI cutoff, while for intermediate- and low-energy electrons the longer pairs also make significant contributions, even though the respective travel times are longer than those of the first pair. The reason is that the longer orbits have higher tunnel ionization rates than the first pair [11]. Thus the higher pairs do modify the detailed shape of the ATI spectrum [10], but this has never been verified in experiments. As mentioned above, an exception occurs near channel closings when many long orbits all interfere constructively [14].

For elliptical polarization, an additional effect becomes relevant. Orbits that start with zero velocity will be driven off by the small component of the elliptically polarized field so that they would never revisit. Hence, they have to start with a compensating nonzero velocity in the direction of the small component that offsets this drift. The larger this velocity, the more suppressed is the contribution of the respective orbit. The nonzero initial velocity has to be especially large for the first pair. Therefore, the longer orbits, which require smaller initial velocities, may become more important and, for large ellipticity, even dominant [17]. The effect has been seen in experiments [8], but a quantitative comparison with theory was not attempted and the relative significance of the longer orbits, compared with the shortest ones, in HATI spectra is still obscure. For NSDI, the significance of longer orbits has been suggested by S-matrix calculations [23] and by classical-trajectory simulations [24]. Their effect on the *total* NSDI yield as a function of the pulse length was addressed in Ref. [25].

The above narrative follows from the analysis of the generalized SFA ionization amplitude from the initial bound state $|\psi_0\rangle$ into the final Volkov state $|\psi_{\mathbf{p}}(t)\rangle$ with momentum $\mathbf{p}$, as described in earlier papers [10,11,26,27],

$$M(\mathbf{p}) = -\int_{-\infty}^{\infty} dt \int_{-\infty}^{t} dt' \langle \psi_{\mathbf{p}}(t)|V U(t,t')V|\psi_0(t')\rangle, \quad (1)$$

where $U(t,t')$ denotes the Volkov time-evolution operator for a free electron in the laser field and V is the atomic potential. The amplitude [Eq. (1)] includes both direct and rescattered electrons. The description of the latter corresponds to the first-order Born approximation for the revisiting electrons. For sufficiently high intensity and low frequency of the laser field, the temporal integrations can be evaluated with high accuracy by the saddle-point method [10]. Each saddle point (t_s, t_s') $(s = 1, 2, \ldots)$ defines an ionization time t_s' and a scattering time t_s, and thereby a "quantum orbit" as discussed above, except that these times have a nonzero imaginary part. It originates from the tunneling process; if we let the ionization potential $I_p = 0$, everything is real. The transition amplitude Eq. (1) can be represented as the coherent superposition of the contributions from all of the quantum orbits, which may add constructively or destructively. In our simulation, for simplicity we will use a zero-range potential as the model potential [14]. For comparison with the experimental data, the calculated photoelectron spectra have to be integrated over the spatiotemporal intensity distribution in the laser focus [28,29].

In Fig. 2(a), we present the calculated focal-averaged photoelectron spectra of Ar in the direction of the major polarization axis for different ellipticities. The calculation qualitatively reproduces various features of the data of Fig. 1(a), especially the ellipticity-independent onset of the plateau. The calculation underestimates the relative yield of the plateau, which is typical for the zero-range potential.

In order to assess the relative contribution of the first and the higher pairs of orbits, in Figs. 1(d)–1(f) we plot the ratios of the yields of several low-energy intervals of the plateau over one high-energy interval as functions of the ellipticity. Specifically, we select four electron-energy ranges in the lower part of the plateau so that each covers two ATI peaks, namely (17.0–20.1), (20.1–23.2), (23.2–26.3), and (26.3–29.4) eV, and form the ratios over the high-energy

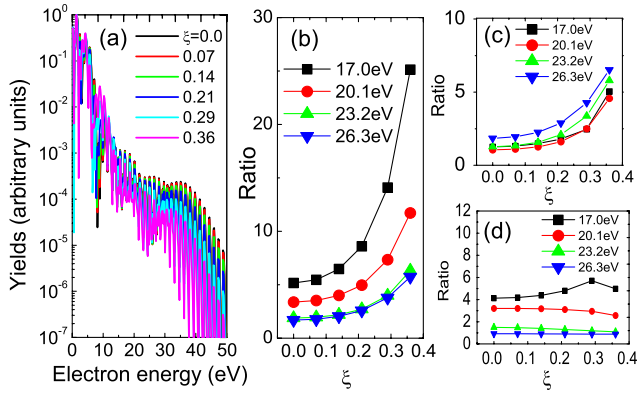

FIG. 2 (color online). (a) The calculated focal-averaged photoelectron spectra of Ar along the major polarization axis for the ellipticities $\xi = 0$, 0.07, 0.14, 0.21, 0.29, and 0.36 from top to bottom. (b) Similar to Fig. 1(d) but for the theoretical calculation, in which the first twenty pairs of quantum orbits are included. (c) Similar to (b), but only the first pair of orbits is considered in the calculation. (d) The ratio of the two ratios displayed in (b) and (c). The laser parameters are chosen as the wavelength of 800 nm and the intensity of 6.2×10^{13} W/cm^2, somewhat below the peak intensity of the experiment [30].

part in the interval (37.0–40.1) eV. In general, for all three noble gas species, i.e., Ar, Kr, and Xe, the ratios exhibit almost the same ellipticity dependence: they increase with increasing ellipticity, especially for $\xi \geq 0.3$. Careful inspection of the ellipticity dependence of the ratios for the various electron energies reveals a crucial point: the lower the electron energy, the faster the ratio increases with increasing ellipticity. We will show below that this observation is closely related to the fact that the longer orbits are more and more favored when the ellipticity of the laser field increases.

In Fig. 2(b) we show the corresponding SFA simulation for argon. We used the saddle-point method and included the contributions of the first 20 pairs of orbits. One finds that the agreement with regard to the ellipticity dependence of the theoretical and the experimental ratios is quite good and essentially all the main features in Fig. 1(d) are reproduced by the calculation displayed in Fig. 2(b). If, however, only the first pair of orbits is considered [see Fig. 2(c)], the ratios come out much too small, especially for low and intermediate electron energies (i.e., 17.0 and 20.1 eV), indicating that the long orbits significantly contribute to the electron yields from linear polarization up to ellipticity 0.36. More importantly, the experimental fact that the ellipticity dependence is stronger for the lower energies (e.g., 17.0 eV) cannot be reproduced unless the longer orbits are included [Fig. 2(c)].

To show this point more clearly, we plot in Fig. 2(d) the ratio between the two ratios of Figs. 2(b) and 2(c) as a function of ellipticity. The higher this ratio is, the larger the contribution of the longer orbits relative to that of the shortest pair. For the lower energies of 17.0 and 20.1 eV, the ratio is much larger than unity, which confirms the significance of the longer orbits. For the electron energy of 17.0 eV, it increases from 4.10 for linear polarization to 5.70 for $\xi = 0.29$ (although followed by a slight decrease for the highest ellipticity of 0.36). This demonstrates the fact that the longer orbits play an increasingly important role with increasing ellipticity. For higher energies (e.g., 20.1 eV), the behavior is different because two additional circumstances complicate the picture: first, the energies E come to lie in the (ellipticity-dependent) cutoff regions of the longer orbits [20] and, second, as becomes clear from Fig. 3, interference may play a vital role in shaping the spectrum.

In order to gain further physical insight into this ellipticity dependence, we present the photoelectron spectra of only the rescattering electrons without focal averaging, for $\xi = 0$ and 0.36, in Figs. 3(a) and 3(b). In addition, the individual contributions of the first, second, and third pair of orbits are separately extracted from the S-matrix calculation, which correspond to those electrons that rescatter upon their first, second, or third return.

For linear polarization [Fig. 3(a)], the first pair is clearly dominant for the electrons with very high kinetic energy, while for intermediate- and low-energy electrons, the second pair also contributes significantly to the HATI electron yield, as discussed above. For an ellipticity of $\xi = 0.36$ as shown in Fig. 3(b) the electron yields of the second pair have become the strongest in the intermediate- and low-energy parts of the plateau. The reason was discussed above: an electron on an orbit of the first pair requires a larger transverse initial momentum in order to return to the ion than an electron on a longer orbit so that its contribution is reduced.

Comparing linear and elliptical polarization (ξ=0.36) one notices that the yield of the first pair drops by almost two orders of magnitude, *much more* than the yield of the second and even the third pair. Therefore, the total electron yield in the intermediate- and low-energy

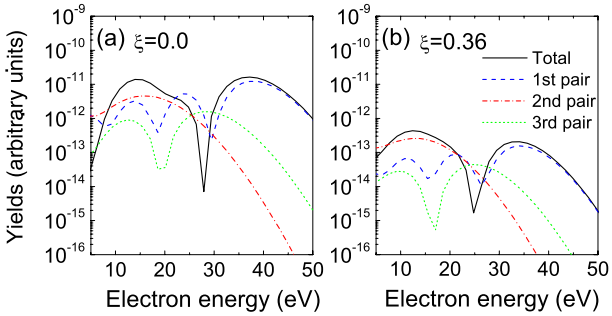

FIG. 3 (color online). Photoelectron spectra along the major polarization axis with only the rescattering electrons, as well as the individual contributions of the first, second, and third pair of the rescattering electrons for (a) linear polarization $\xi = 0$ and (b) elliptical polarization $\xi = 0.36$. The parameters are the same as in Fig. 2. For details, see the text.

regime drops more slowly than in the high-energy regime ($E \gtrsim 25$ eV). The consequence is that the ratios shown in Figs. 1(d) and 2(b) increase more strongly with the ellipticity in the former case than in the latter.

In summary, we experimentally studied the ATI spectra of the noble gases Ar, Kr, and Xe along the major polarization axis in intense elliptically polarized laser pulses. With continuously increasing ellipticity, we found that the electron yields in the low-energy part of the ATI plateau drop more slowly than those in the high-energy part. This is attributed to the ellipticity dependence of the first pair as opposed to that of the higher pairs of quantum orbits. Namely, the cutoffs of all pairs recede at about the same rate with increasing ellipticity. However, the magnitude of the contribution of the first pair drops much faster than those of the longer orbits. Therefore, with increasing ellipticity the contribution of the first pair decreases. Because, however, the first pair has the highest cutoff, it remains dominant in the upper part of the plateau but with a much reduced yield. Comparing theory and data we concluded that qualitative agreement can only be obtained by including the contributions of the longer orbits. Moreover, our analysis reveals that with increasing laser ellipticity the contribution of the longer orbits becomes more and more important.

This work is supported by the National Basic Research Program of China (Grants No. 2013CB9222001 and No. 2011CB8081002) and by NNSF of China (Grants No. 10925420, No. 10904162, No. 11074026, No. 11174330, No. 11134010, and No. 11274050).

*xjliu@wipm.ac.cn
†chen_jing@iapcm.ac.cn

[1] P. Agostini, F. Fabre, G. Mainfray, G. Petite, and N. K. Rahman, Phys. Rev. Lett. **42**, 1127 (1979).
[2] P. B. Corkum, Phys. Rev. Lett. **71**, 1994 (1993).
[3] G. G. Paulus, W. Nicklich, H. Xu, P. Lambropoulos, and H. Walther, Phys. Rev. Lett. **72**, 2851 (1994); H. Kang *et al.*, Phys. Rev. Lett. **104**, 203001 (2010).
[4] M. Ferray, A. L'Huillier, X. F. Li, L. A. Lompré, G. Mainfray, and C. Manus, J. Phys. B **21**, L31 (1988); A. D. Shiner, B. E. Schmidt, C. Trallero-Herrero, H. J. Wörner, S. Patchkovskii, P. B. Corkum, J.-C. Kieffer, F. Légaré, and D. M. Villeneuve, Nat. Phys. **7**, 464 (2011).
[5] B. Walker, B. Sheehy, L. F. DiMauro, P. Agostini, K. J. Schafer, and K. C. Kulander, Phys. Rev. Lett. **73**, 1227 (1994); C. F. de Morisson Faria and X. Liu, J. Mod. Opt. **58**, 1076 (2011); W. Becker, X. Liu, P. J. Ho, and J. H. Eberly, Rev. Mod. Phys. **84**, 1011 (2012).
[6] T. Nubbemeyer, K. Gorling, A. Saenz, U. Eichmann, and W. Sandner, Phys. Rev. Lett. **101**, 233001 (2008).
[7] M. Lewenstein, K. C. Kulander, K. J. Schafer, and P. H. Bucksbaum, Phys. Rev. A **51**, 1495 (1995).
[8] P. Salières *et al.*, Science **292**, 902 (2001).
[9] M. Lewenstein, P. Salières, and A. L'Huillier, Phys. Rev. A **52**, 4747 (1995).
[10] R. Kopold, W. Becker, and M. Kleber, Opt. Commun. **179**, 39 (2000).
[11] W. Becker, F. Grasbon, R. Kopold, D. B. Milošević, G. G. Paulus, and H. Walther, Adv. At. Mol. Opt. Phys. **48**, 35 (2002).
[12] J. Tate, T. Auguste, H. G. Muller, P. Salières, P. Agostini, and L. F. DiMauro, Phys. Rev. Lett. **98**, 013901 (2007); A. Zaïr *et al.*, Phys. Rev. Lett. **100**, 143902 (2008).
[13] C. M. Heyl, J. Güdde, U. Höfer, and A. L'Huillier, Phys. Rev. Lett. **107**, 033903 (2011).
[14] G. G. Paulus, F. Grasbon, H. Walther, R. Kopold, and W. Becker, Phys. Rev. A **64**, 021401(R) (2001).
[15] S. V. Popruzhenko, Ph. A. Korneev, S. P. Goreslavski, and W. Becker, Phys. Rev. Lett. **89**, 023001 (2002).
[16] D. B. Milošević, E. Hasović, M. Busuladžić, A. Gazibegović-Busuladžić, and W. Becker, Phys. Rev. A **76**, 053410 (2007).
[17] R. Kopold, D. B. Milošević, and W. Becker, Phys. Rev. Lett. **84**, 3831 (2000).
[18] N. Dudovich, J. Levesque, O. Smirnova, D. Zeidler, D. Comtois, M. Yu. Ivanov, D. M. Villeneuve, and P. B. Corkum, Phys. Rev. Lett. **97**, 253903 (2006).
[19] A. N. Pfeiffer, C. Cirelli, M. Smolarski, R. Dörner, and U. Keller, Nat. Phys. **7**, 428 (2011).
[20] For HHG, ellipticity-dependent cutoffs of the first three pairs of orbits were derived by D. B. Milošević, J. Phys. B **33**, 2479 (2000). For small ellipticity, they are approximately the linear-polarization cutoffs divided by $(1 + \xi^2)$. For HATI, corresponding results are not available, but it is reasonable to assume the same approximate dependence.
[21] D. B. Milošević, W. Becker, M. Okunishi, G. Prümper, K. Shimada, and K. Ueda, J. Phys. B **43**, 015401 (2010).
[22] R. Kopold, W. Becker, and D. B. Milošević, J. Mod. Opt. **49**, 1987 (2002).
[23] N. I. Shvetsov-Shilovski, S. P. Goreslavski, S. V. Popruzhenko, and W. Becker, Phys. Rev. A **77**, 063405 (2008).
[24] X. Wang and J. H. Eberly, New J. Phys. **12**, 093047 (2010).
[25] V. R. Bhardwaj, S. A. Aseyev, M. Mehendale, G. L. Yudin, D. M. Villeneuve, D. M. Rayner, M. Yu. Ivanov, and P. B. Corkum, Phys. Rev. Lett. **86**, 3522 (2001).
[26] A. Lohr, M. Kleber, R. Kopold, and W. Becker, Phys. Rev. A **55**, R4003 (1997).
[27] D. B. Milošević and F. Ehlotzky, Phys. Rev. A **58**, 3124 (1998).
[28] E. Hasović, M. Busuladžić, A. Gazibegović-Busuladžić, D. B. Milošević, and W. Becker, Laser Phys. **17**, 376 (2007).
[29] R. Kopold, W. Becker, M. Kleber, and G. G. Paulus, J. Phys. B **35**, 217 (2002).
[30] For comparison with the experimental data, a laser intensity slightly lower than the one estimated for the experiment was adopted. This has been standard practice in SFA calculations, see, e.g., Ref. [21].